MFO Ptimized Fractional Order Based Controller
on Power System Stability

Bidyadhar Rout[*], Bibhuti Bhusan Pati

Department of Electrical Engineering, Veer Surendra Sai University of Technology, Burla, Odisha, India.

Abstract

This paper presents a novel idea of designing the Fractional-Order PID (FOPID) type static synchronous series compensator (SSSC). A power system stabilizer(PSS) is installed to enhance the system transient stability by damping the oscillations. Also the superiority of the proposed method is verified by comparing with conventional PI, PI-PD and PID controllers. The determination of the controller parameters has been considered as an optimization problem using Moth Fly Optimization (MFO). It is shown that MFO is more effective as well as giving robust response than Differential Evolution (DE) optimization. The superiority of the controller is tested on Single-Machine Infinite-Bus (SMIB) power systemat various operating conditions and fault locations.

1. Introduction

Recently, the using of MFO optimization technique is based on the motion of a moth in a transverse orientation for navigation. It keeps a fixed angle with respect to the moon or the flame. The superiority of the Moth Fly Optimization (MFO) algorithm over Firefly Algorithm (FA) and other algorithms have been reported in many researches [1]. This work has focussed on the application of the MFO algorithm to a typical SMIB power system.

In a power system, the synchronous series compensator (SSSC), is very effective in damping the electromechanical oscillations along with power flow control. It consists of voltage source self-commutated switching converters which synthesises the three phase voltages (in quadrature) with line current to establish the compensation of the power system voltage imbalance [2-6]. In dynamic state; SSSC mainly controls damping of oscillations by injecting the series voltage to the line [3]. To improve the system dynamic performance, an external control loop is added to SSSC which consists of a controller changing the series injected voltage during transient period [4-6]. Such a stabiliser is commonly called as lead lag type SSSC damping controller. The synchronizing torque, damping torque and transient stability limit for both small signal as well as for transient stability are successfully improved with real power in lead-lag (LL) based SSSC damping controller and PSS design [6-8].

It is well known that the conventional controller design methods are not attractive enough for robust stability, due to computational burden, more time consuming, and slow convergence and moreover, the controller parameters are trapped to their local minima and not optimal. Therefore, various optimization methods such as particle swarm optimization (PSO), Differential Evolution (DE) etc.[2, 9-11] are extensively used for tuning PSS and auxiliary controller based SSSC controller parameters[2, 11-13].

---

* Corresponding author. Email address: bdr23@rediffmail.com, bbpati_ee@vssut.ac.in

Because of its robustness and simple structure, the proportional integral derivative (PID) controllers have been largely implemented. [5-7, 14-15]. Since, there are difficulties in finding the mathematical model as well as determination of parameters of PID controller in complex/nonlinear higher order power systems, artificial intelligence techniques have been used [14-17]. In this work MFO optimized controller parameters have been analyzed.

In this investigation, the fractional PID type SSSC controller will be used and the results will be compared with other conventional controllers such as PI type, PI-PD type, and PID type SSSC controllers to show the robustness of the damping at same and different operating conditions for the proposed SMIB power system. The parameters of fractional PID type SSSC and PSS controllers will be simultaneously optimized by the proposed MFO algorithm [1, 16-18].

2. System Investigated

The robustness of damping performances has been assessed for the co-ordinately designed controllers and is tested in a SMIB system as shown in Fig. 1 [4-9, 19]. This setup contains a generator connected to an infinite-bus through a double circuit (DC) transmission line. The generator is provided with the SSSC, and excitation system along with PSS. The SSSC is connected in series in between Bus-1 and Bus-2 through coupling transformer. A line transformer T links to the generator and Bus-1 where as Bus-2 and Bus-3 are connected through DC transmission lines. V_T and V_B are the voltages at the generator terminal and infinite-bus respectively. V_1 and V_2 are the bus voltages at Bus-1 and Bus-2 respectively as shown. Current I is the line current, P_{L1} is the real power flowing in one of the DC transmission line, where the three phase fault is to be created and P_L is the tie line active power flowing in a transmission line. Fig. 1 shows the model power system is developed by using Matlab/Simulink. All the relevant parameters of this system are can be found in [13]. The use of PSS can also be described in a similar way[5-7].
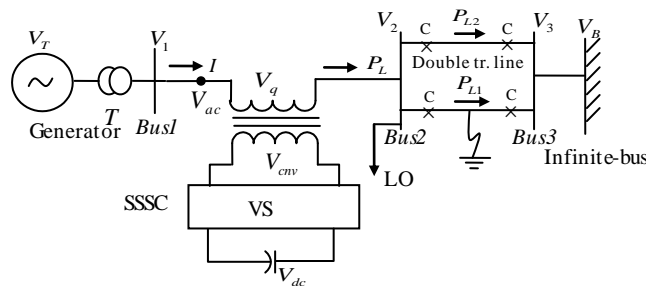

Fig. 1 The Single Machine Infinite Bus (SMIB) Power System with a SSSC[2-3]

2.1. System modelling

The SMIB nonlinear dynamic model deals with the transient analysis [1-5]. The speed deviation is the input to the controller. It is the remote signal from the fault location. The following mechanical dynamics are taken for the proposed system analysis.

$$\frac{d}{dt}\omega_r = \frac{1}{J}(P_e - B\omega_r - P_m) \tag{1}$$

$$\frac{d}{dt}\theta = \omega_r \tag{2}$$

where ω_r and θ represent the angular speed and the rotor angle as state variables of the generator, P_e and P_m are the electrical output and mechanical input power respectively, J and B represent inertia and the coefficient of viscous friction of the rotor respectively. Detail mathematical expression interlinking the system state variables are described in [9-14].

2.2. Structure of SSSC and control system

As discussed, SSSC is composed of a three-phase voltage source converter (VSC), a series coupling transformer, a dc capacitor V_{dc} , and AC and dc voltage regulators[2-7]. The objective of using VSC is to convert a dc voltage into three phase AC voltage with fundamental frequency which is to be fed into line and in phase quadrature (independent from line current) with the line current I. The injected AC voltage V_q changes in its magnitude due to variable fictitious capacitive or inductive reactance during transient conditions. This voltage controls the active power flow efficiently and damps out the power swings. In capacitive mode, V_{cnv} is greater than V_{ac} and it supplies active and reactive power to power system and in inductive mode, V_{cnv} is lower than V_{ac}. The control device maintains the voltage profile of transmission line unchanged by controlling the converter voltage[2, 5, 19].

2.3. Fractional order PID (FOPID) controller

Widespread interest in FOPID controller has attracted many researchers in power system to provide insight into the transient stability study. It is represented by $PI^\lambda D^\mu$ which provides added degree of freedom for designing controller gains (K_P, K_I, K_D) where the orders of integral and derivative are real numbers not necessarily only integers. The FOPID controller has the merit of providing an extra degree of freedom and is less sensitive to parameter variation compared to a classical PID controller [17]. The transfer function of such FOPID controller:

$$G_c(s) = (K_P + \frac{K_I}{s^\lambda} + K_D s^\mu) \tag{3}$$

3. The Structures of Various Controllers

The structures of various types of controllers e.g. PI type, PI-PD type, PID type and the FOPID controller have been described in the following section for both the SSSC as well as PSS installation in the example system.

3.1 PI type SSSC controller structure

Fig. 2 shows the block diagram of PI type SSSC controller structure. Here K_p is the proportional gain and K_I is the integral gain. The PI block is connected to a washout block(for high pass filter action) followed by a two stage Lead Lag compensation block. The wash out block with time constant T_W make it sure that there is no steady state error of the voltage reference due to the speed deviation Δw. Time constant T_W is not critical and may be in the range of 1 to 20 sec [12]. Here, $T_W = 10s$ is taken into consideration. As the input signal (i.e. Δw) to the controller is remote signal, the sensor time with transmission time delay $T_{TD} = 65ms$ is provided at the input to the controller.
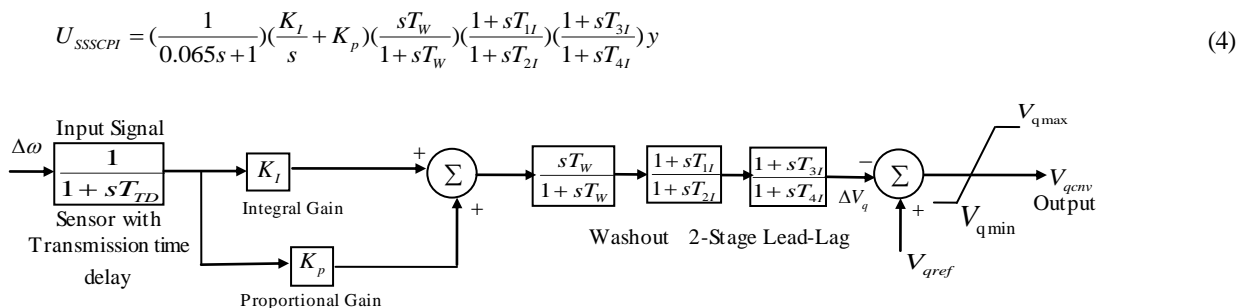
$$U_{SSSCPI} = (\frac{1}{0.065s+1})(\frac{K_I}{s} + K_p)(\frac{sT_W}{1+sT_W})(\frac{1+sT_{1I}}{1+sT_{2I}})(\frac{1+sT_{3I}}{1+sT_{4I}})y \tag{4}$$

Fig. 2 Structure of PI type SSSC damping controller

3.2 PI type PSS controller structure

$$U_{PSSPI} = (\frac{1}{0.015s+1})(\frac{K_{I1}}{s} + K_{p1})(\frac{sT_W}{1+sT_W})(\frac{1+sT_{11I}}{1+sT_{21I}})(\frac{1+sT_{31I}}{1+sT_{41I}})y \tag{5}$$
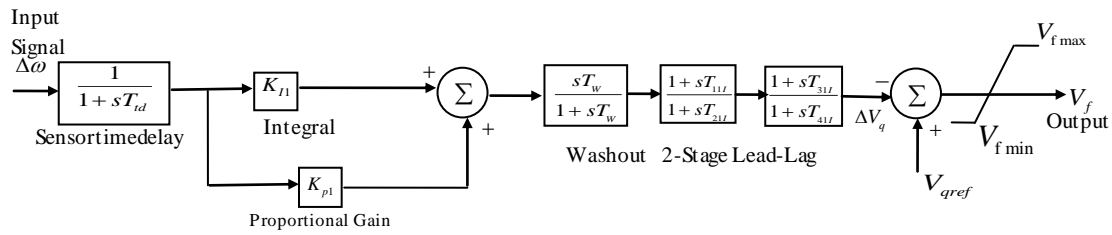
Fig. 3 Structure of PI type PSS damping controller

The controller gains and time constant parameters of PI type SSSC and PSS controller must be tuned for achieving best performances. A first order sensor with sensor time delay $T_{td} = 15ms$ is chosen by this controller for sensing the low frequency speed deviation Δw during disturbances[8].

3.3. PI-PD type SSSC controller structure

Improved system performance is expected with the cascade control system. Fig. 4 shows a cascade PI-PD controller for SSSC controller [7-10]. The performances are improved by putting a first order filter with tuning pole and filter constant N = 100 Similar PI-PD type PSS controller structure can be used for analysing the behaviour of PSS damping controller.

$$U_{SSSCPI-PD} = (\frac{1}{0.065s+1})(\frac{K_{I2}}{s} + K_{p2})(K_{d3}\frac{sN}{s+N} + K_{p3})(\frac{sT_W}{1+sT_W})(\frac{1+sT_{1ID}}{1+sT_{2ID}})(\frac{1+sT_{3ID}}{1+sT_{4ID}})y \qquad (6)$$
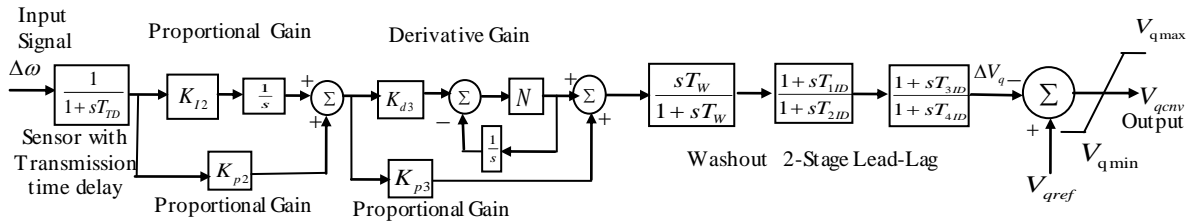

Fig. 4 Structure of PI-PD type SSSC damping controller[19]

3.4 PID type SSSC controller structure

Conventional PID type SSSC controller structure is taken for comparing the responses with the previous controller structures. For the conventional PID type SSSC damping controller, the output is:

$$U_{SSSCPID} = (\frac{1}{0.065s+1})(\frac{K_{Ic}}{s} + K_{dc}\frac{sN}{s+N} + K_{pc})(\frac{sT_W}{1+sT_W})(\frac{1+sT_{1c}}{1+sT_{2c}})(\frac{1+sT_{3c}}{1+sT_{4c}})y \qquad (7)$$
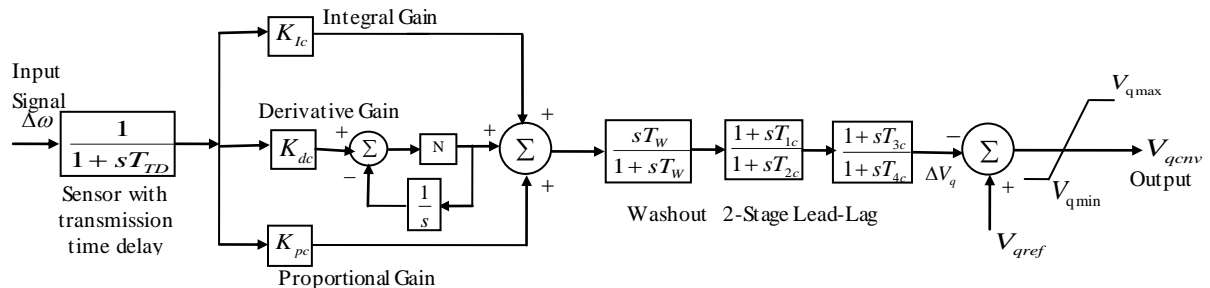

Fig. 5 Structure of conventional PID type SSSC controller

Similar PID type PSS controller structure can be used for analysing the behavious of PSS damping controllers.

Here, K_{pc}, K_{Ic} K_{dc}, K_{p1c}, K_{I1c}, K_{d1c}, T_{1c}, T_{2c}, T_{3c}, T_{4c}, T_{11c}, T_{21c}, T_{31c}, T_{41c} are gains and time constant parameters of PID type SSSC and its PID type PSS controller that are to be tuned for achieving best performances[20].

3.5 FOPID type SSSC controller structure

For fractional type SSSC controller, the output is:

$$U_{SSSCFPID} = (\frac{1}{0.065s+1})(\frac{K_I}{s^\lambda} + K_d s^\mu + K_p)(\frac{sT_W}{1+sT_W})(\frac{1+sT_1}{1+sT_2})(\frac{1+sT_3}{1+sT_4})y \tag{8}$$

The proposed fractional PID type SSSC is a supplementary damping controller whose structure is shown in Fig. 6, is to modulate the SSSC injected voltage V_q. Similar FOPID type PSS controller structure has been applied to analyse the damping behaviour. A first order sensor with sensor time delay T_{td}=15ms is taken with this controller for sensing the low frequency speed deviation Δw during disturbances. The controller gain $K_p, K_I K_d, K_{p1}, K_{I1}, K_{d1}$ and the time constant values like $T_1, T_2, T_3, T_4, T_{11}, T_{21}, T_{31}, T_{41}, \lambda, \mu, \lambda_1$ and μ_1 are to be tuned optimally [21].
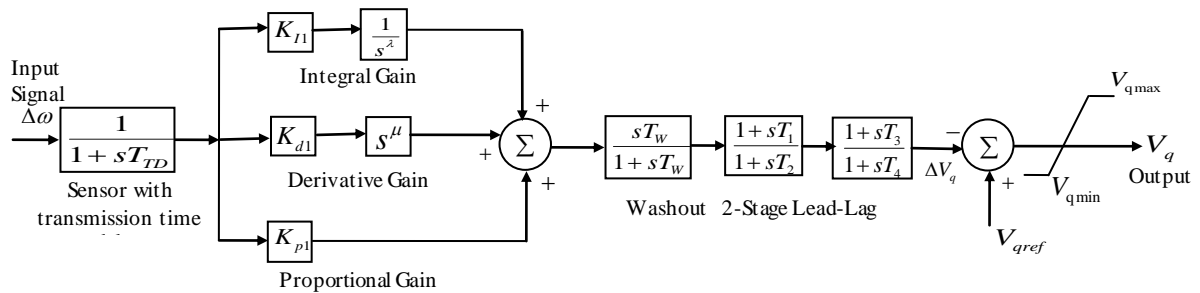

Fig. 6 Structure of FOPID type SSSC damping controller

3.6. Control Objectives

Power system after passing through a large disturbance exhibit oscillation which can be minimized or quenched by application of SSSC and this improves the stability. These oscillations are observed in terms of power angle, rotor speed and line power. The objective is to reduce any one or all of these deviations. In the present study, an integral time absolute error (ITAE) of the speed signals corresponding to the remote modes of oscillations is taken as the objective function. The objective function is expressed as

$$J = \int_{t=0}^{t=t_{sim}} |\Delta w|.t.dt \tag{9}$$

where t_{sim} is the simulation time period. The percentage overshoot and the settling time can be improved by minimizing this objective function. The constraints here are the parameters of SSSC controller. The optimisation problem can be as the following optimization problem: Minimizing J, and subject to

For PI type SSSC damping controller

$$K_p^{min} \le K_p \le K_p^{max}, K_I^{min} \le K_I \le K_I^{max} \tag{10}$$

$$T_{1I}^{min} \le T_{1I} \le T_{1I}^{max}, T_{2I}^{min} \le T_{2I} \le T_{2I}^{max}, T_{3I}^{min} \le T_{3I} \le T_{3I}^{max}, T_{4I}^{min} \le T_{4I} \le T_{4I}^{max} \tag{11}$$

For PI type PSS controller

$$K_{p1}^{min} \le K_{p1} \le K_{p1}^{max}, K_{I1}^{min} \le K_{I1} \le K_{I1}^{max} \tag{12}$$

$$T_{11I}^{min} \le T_{11I} \le T_{11I}^{max}, T_{21I}^{min} \le T_{21I} \le T_{21I}^{max}, T_{31I}^{min} \le T_{31I} \le T_{31I}^{max}, T_{41I}^{min} \le T_{41I} \le T_{41I}^{max} \tag{13}$$

For PI-PD type SSSC damping controller

$$K_{p2}^{\min} \le K_{p2} \le K_{p2}^{\max}, K_{I2}^{\min} \le K_{I2} \le K_{I2}^{\max}, K_{p3}^{\min} \le K_{p3} \le K_{p3}^{\max}, K_{d3}^{\min} \le K_{d3} \le K_{d3}^{\max} \tag{14}$$

$$T_{1ID}^{\min} \le T_{1ID} \le T_{1ID}^{\max}, T_{2ID}^{\min} \le T_{2ID} \le T_{2ID}^{\max}, T_{3ID}^{\min} \le T_{3ID} \le T_{3ID}^{\max}, T_{4ID}^{\min} \le T_{4ID} \le T_{4ID}^{\max} \tag{15}$$

For PI-PD type PSS controller

$$K_{p12}^{\min} \le K_{p12} \le K_{p12}^{\max}, K_{I12}^{\min} \le K_{I12} \le K_{I12}^{\max}, K_{p13}^{\min} \le K_{p13} \le K_{p13}^{\max}, K_{d13}^{\min} \le K_{d13} \le K_{d13}^{\max} \tag{16}$$

$$T_{11ID}^{\min} \le T_{11ID} \le T_{11ID}^{\max}, T_{21ID}^{\min} \le T_{21ID} \le T_{21ID}^{\max}, T_{3ID}^{\min} \le T_{31ID} \le T_{31ID}^{\max}, T_{41ID}^{\min} \le T_{41ID} \le T_{41ID}^{\max} \tag{17}$$

For PID type SSSC damping controller

$$K_{pc}^{\min} \le K_{pc} \le K_{pc}^{\max}, K_{Ic}^{\min} \le K_{Ic} \le K_{Ic}^{\max}, K_{dc}^{\min} \le K_{dc} \le K_{dc}^{\max} \tag{18}$$

$$T_{1c}^{\min} \le T_{1c} \le T_{1c}^{\max}, T_{2c}^{\min} \le T_{2c} \le T_{2c}^{\max}, T_{3c}^{\min} \le T_{3c} \le T_{3c}^{\max}, T_{4c}^{\min} \le T_{4c} \le T_{4c}^{\max} \tag{19}$$

For PID type PSS controller

$$K_{p1c}^{\min} \le K_{p1c} \le K_{p1c}^{\max}, K_{I1c}^{\min} \le K_{I1c} \le K_{I1c}^{\max}, K_{d1c}^{\min} \le K_{d1c} \le K_{d1c}^{\max} \tag{20}$$

$$T_{11c}^{\min} \le T_{11c} \le T_{11c}^{\max}, T_{21c}^{\min} \le T_{21c} \le T_{21c}^{\max}, T_{31c}^{\min} \le T_{31c} \le T_{31c}^{\max}, T_{41c}^{\min} \le T_{41c} \le T_{41c}^{\max} \tag{21}$$

For FOPID type SSSC damping controller

$$K_p^{\min} \le K_p \le K_p^{\max}, K_I^{\min} \le K_I \le K_I^{\max}, K_d^{\min} \le K_d \le K_d^{\max} \tag{22}$$

$$T_1^{\min} \le T_1 \le T_1^{\max}, T_2^{\min} \le T_2 \le T_2^{\max}, T_3^{\min} \le T_3 \le T_3^{\max}, T_4^{\min} \le T_4 \le T_4^{\max} \tag{23}$$

$$\mu^{\min} \le \mu \le \mu^{\max} \tag{24}$$

For FOPID type PSS controller

$$K_{p1}^{\min} \le K_{p1} \le K_{p1}^{\max}, K_{I1}^{\min} \le K_{I1} \le K_{I1}^{\max}, K_{d1}^{\min} \le K_{d1} \le K_{d1}^{\max} \tag{25}$$

$$T_{11}^{\min} \le T_{11} \le T_{11}^{\max}, T_{21}^{\min} \le T_{21} \le T_{21}^{\max}, T_{31}^{\min} \le T_{31} \le T_{31}^{\max}, T_{41}^{\min} \le T_{41} \le T_{41}^{\max} \tag{26}$$

$$\lambda_1^{\min} \le \lambda_1 \le \lambda_1^{\max} \tag{27}$$

In this investigation DE and MFO techniques are applied to search for optimal set of SSSC-based damping controller parameters. A brief introduction of Moth-Flame Optimization(MFO) technique is described in the next section.

4. Overview of MFO

This has been widely used in many such important applications and giving very promising results. It is briefly discussed in this section to make the paper self-content. The behavior of the fly is mathematically modeled by an algorithm called MFO algorithm, assuming the candidate solutions are moths and the problem's variables are the position of moths in the space. This algorithm is a population-based algorithm, where the set of moths is represented in a matrix M consisting of the array as their corresponding fitness values. The flame matrix is represented by where the array of F also stores the fitness values.

The initial point, final point of the flame and range of fluctuation of spiral in the search space are required for the spiral movement of the moth which is expressed as

$$M_i = S(M_i, F_j) \tag{28}$$

where M_i indicates the i-th moth position, F_i indicates the j-th flame position. Knowing the initial point, final point of the flame and range of fluctuation of spiral in the search space, the spiral movement of the moth is expressed as

$$S(M_i, F_j) = D_i.e^{bt}.Cos(2\pi t) + F_j \tag{29}$$

where t is a random number [-1, 1], and D_i is the distance of the ith moth for the jth flame. And is calculated as:

$$D_i = \left| F_j - M_i \right| \tag{30}$$

where M_i indicates the ith moth, F_j indicates the jth flame, and D_i indicates the distance of the ith moth for the jth flame which is to be minimized.

The next position of a moth is defined with respect to a flame following Eq. (29). The t-parameter in the equation which closeness to flame equals to -1 and 1 implies farther to the flame. Due to change of order of flames and revision of moth's position at each iteration, the exploitation of the promisingly best solutions is obtained through an adaptive mechanism proposed by using the number of flames.

$$flame\_no = round(N - l * \frac{N-1}{T}) \tag{31}$$

where N and T represents maximum no. of flames, and iterations respectively, l is the current number of iteration. The algorithm flow chart is shown in Fig. 7.
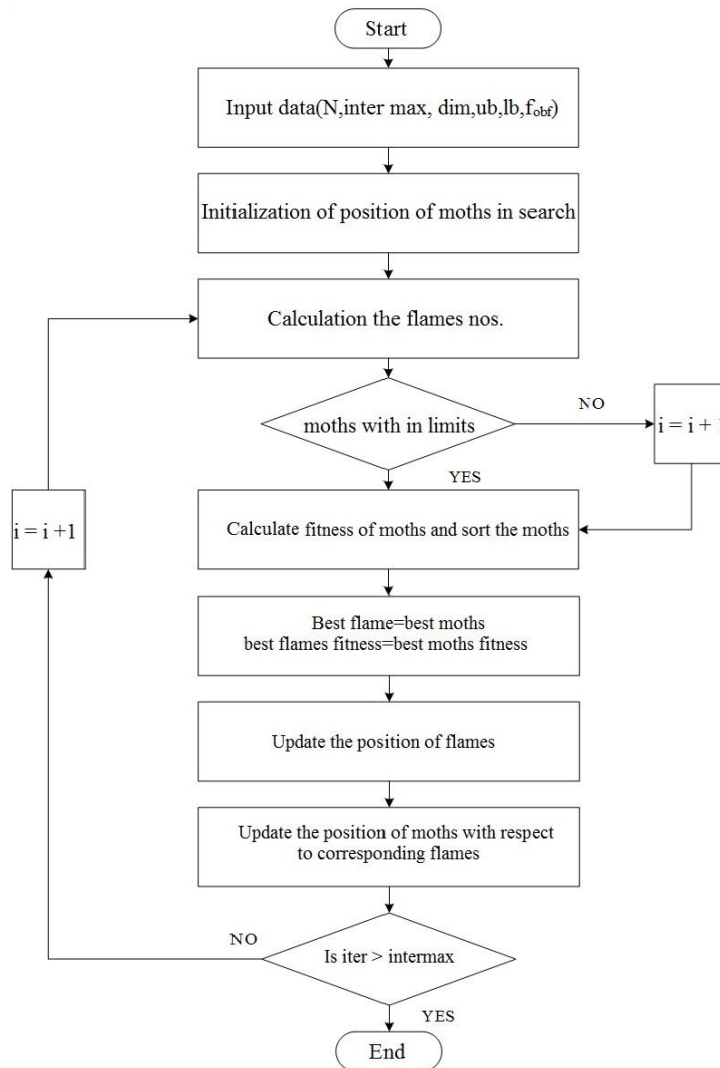

Fig. 7 Flow chart of the proposed MFO algorithm[1]

5. Simulation Results And Analysis

The system described in Fig. 1 is simulated in MATLAB under three phase disturbance at different locations. The objective function is minimised by tuning the fractional PID type SSSC and PSS controller parameters with MFO and compared with DE algorithm as shown in Table 4. The result is compared with PI type SSSC and PSS (Table 1), PI-PD type SSSC and PSS (Table 2), PID type SSSC and PSS damping controllers (Table 3). The robustness and effectiveness of the proposed FPID type SSSC and PSS is verified at various generator loadings. After hundred iterations, the optimized parameters along with the performance indices of ITAE are noted down from both DE and MFO algorithms. The simulation results for all controllers are shown in Figs. 8-11.

5.1. Case-1: PI type SSSC-PSS Controller

The nominal loading $(0.8 p.u, \delta_0 = 48.48^0)$, is the Self-cleared between Bus-2 and Bus-3. A three phase line fault is created at one of the double section line between Bus-2 and Bus-3 at t = 1s in SMIB power system for nominal loading and self-cleared for 5 cycles. The post fault oscillation are damped out through MFO and DE optimised PI type SSSC and PSS controller and the effective results are found through MFO optimized parameters. The parameters comparison is shown in table-1 and the simulation responses are shown in Figs. 8-11 with the legend "PI type SSSC (MFO)" with a solid green line and "PI type SSSC (DE)" with dotted pink line.

Table 1 DE and MFO tuned optimal parameter of PI type SSSC and PSS controller at nominal loading $(0.8 p.u, \delta_0 = 48.48^0)$

Optimisation	Controller	Controller Parameters						ITAE *10e-3
DE	PI type SSSC	K_p	K_I	T_{1I}	T_{2I}	T_{3I}	T_{4I}	3.8
		195.403	12.9818	0.5881	0.6896	1.4308	1.9145	
	PI type PSS	K_{p1}	K_{I1}	T_{11I}	T_{21I}	T_{31I}	T_{41I}	
		21.0723	11.0937	1.2773	1.6716	0.0146	1.9139	
MFO	PI type SSSC	K_p	K_I	T_{1I}	T_{2I}	T_{3I}	T_{4I}	3.7
		158.3171	6.3069	1.7456	1.9974	0.4081	0.8803	
	PI type PSS	K_{p1}	K_{I1}	T_{11I}	T_{21I}	T_{31I}	T_{41I}	
		1.7652	11.4863	1.1977	0.0010	1.7735	1.6014	
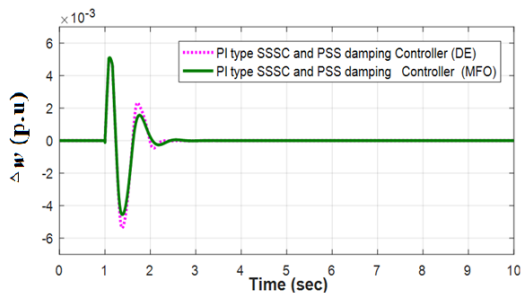
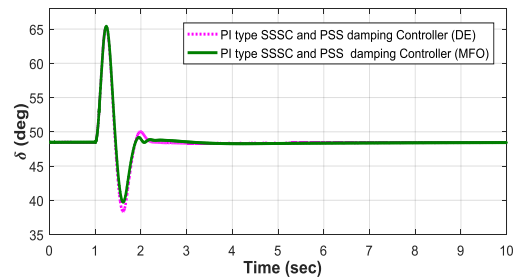Fig. 8 Speed deviation Δw in p.u

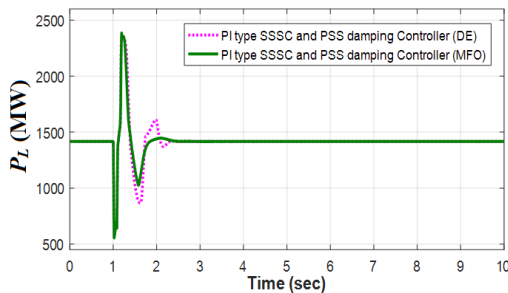

Fig. 9 Rotor angle δ in in degree

Fig. 10 The line active power P_L in MW

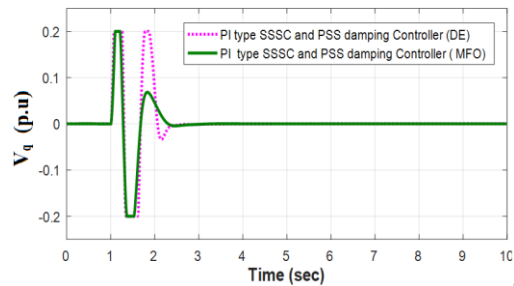
Fig. 11 SSSC-injected voltage V_q in p.u

5.2. Case-2:PI-PD type SSSC and PSS controller

The nominal loading $(0.8 p.u, \delta_0 = 48.48^0)$, is the self-cleared at between Bus-2 and Bus-3. Table 2 shows the optimised parameters with both DE and MFO for PI-PD type SSSC and PSS controller during three phase Bus-2 and Bus-3 and self-cleared condition for 5 cycles. The effective responses are analysed in Fig.9. It is observed in Fig. 12-15 for speed deviation, tie line power and terminal voltage. The improvement of settling time and decrement of overshot of transient responses are observed in this MFO optimised PI-PD type SSSC and PSS controller more effectively than controller.

Table 2 DE and MFO tuned optimal parameter of PI-PD type SSSC and PSS controller with nominal

loading $(0.8 p.u, \delta_0 = 48.48^0)$ line outage

| Optimisation	Controller	Controller Parameters								ITAE *10e-3
DE	PI-PD type SSSC	K_{p2}	K_{I2}	K_{p3}	K_{d3}	T_{1ID}	T_{2ID}	T_{3ID}	T_{4ID}	4.2
		8.9062	7.7024	91.2532	32.1083	0.9168	1.7648	0.2907	0.7114	
	PI-PD type PSS	K_{p12}	K_{I12}	K_{p13}	K_{d13}	T_{11ID}	T_{21ID}	T_{31ID}	T_{41ID}	
		55.8208	17.3684	15.7298	12.5812	0.8535	1.4744	0.2200	1.4390	
MFO	PI-PD type SSSC	K_{p2}	K_{I2}	K_{p3}	K_{d3}	T_{1ID}	T_{2ID}	T_{3ID}	T_{4ID}	2.9
		0.9990	8.2677	102.8586	92.6227	1.0339	0.6070	0.9069	1.6722	
	PI-PD type PSS	K_{p12}	K_{I12}	K_{p13}	K_{d13}	T_{11ID}	T_{21ID}	T_{31ID}	T_{41ID}	
		0.9990	0.0000	99.87	9.3844	0.0001	1.9974	0.0001	1.8503	
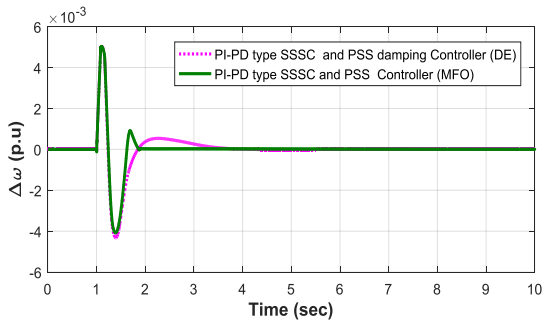
Fig. 12 Speed deviation
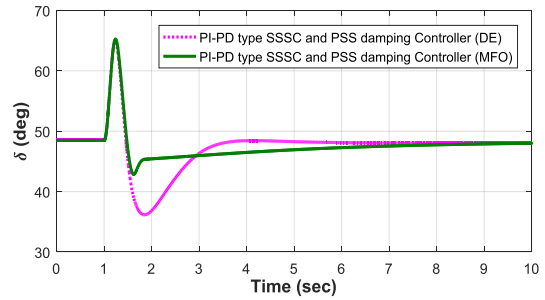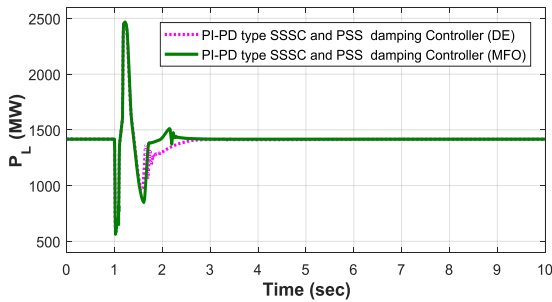

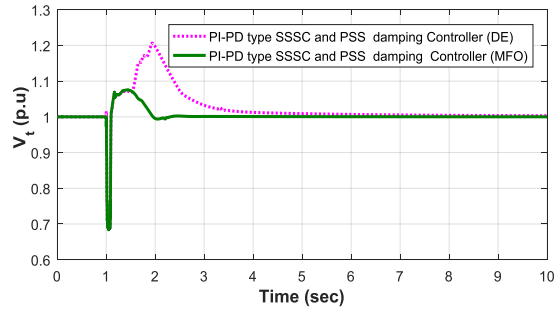Fig. 13 Rotor angle in degree

Fig. 14 Tie line active power

Fig. 15 Terminal voltage

5.3. Case-3: PID type SSSC and PSS controller

The nominal loading at ($P_e = 0.8, \delta_0 = 48.4^0$), is the line outage Bus-2 and Bus-3. PID type SSSC and PSS controller has also been tested with this SMIB system at line outage disturbance condition at same fault location between Bus-2 and Bus-3.The three phase line outage disturbance is done at t = 1s for 5 cycles and the effective responses are analysed in Figs. 16-18 following optimized controller parameters in table-3. It is found that, the responses for PID type SSSC and PSS controller are better as compared to PI and PI-PD type SSSC and PSS controller. The MFO optimized controller parameters of PID type SSSC and PSS gives better responses than the DE tuned PID type SSSC and PSS controller. The settling time in PID type SSSC is significantly improved than PI and PI-PD type SSSC controllers.
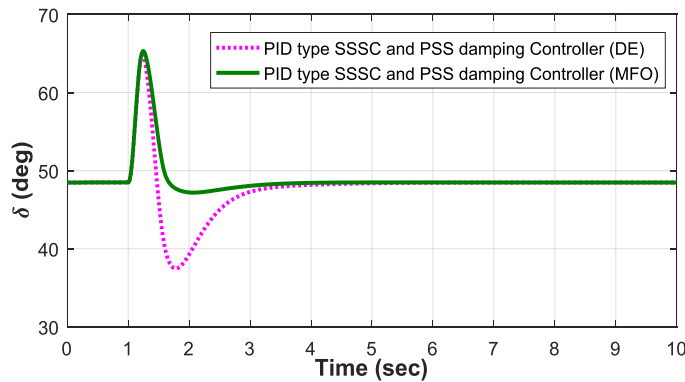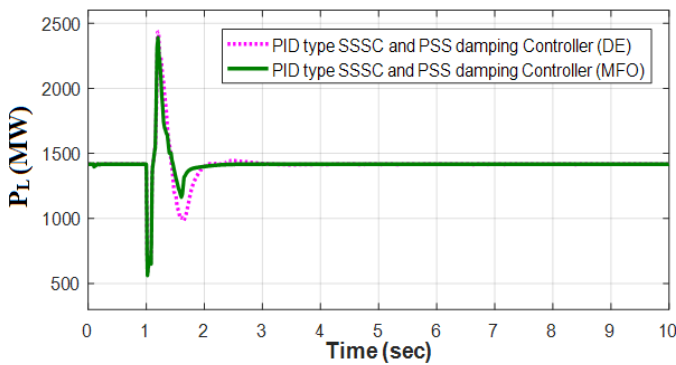
Fig. 16 Speed deviation
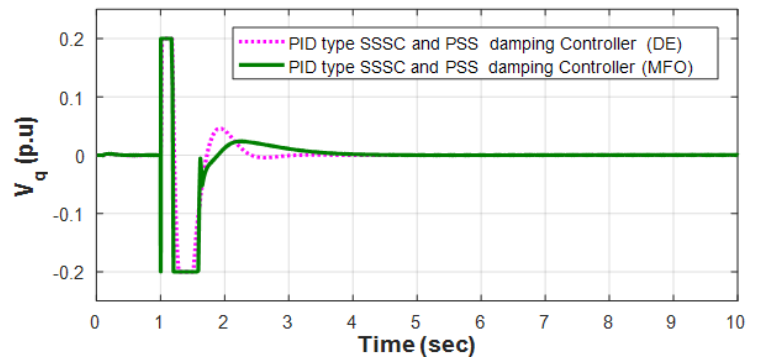

Fig. 17 The line active power

Fig. 18 SSSC-injected voltage

Table 3 DE and MFO tuned optimal parameter of PID type SSSC and PSS controller with nominal loading (0.8p $(0.8 p.u, \delta_0 = 48.48^0)$, line outage

Optimisation	Controller	Controller Parameters							ITAE *10e-3
DE	PID type SSSC	K_{pc}	K_{Ic}	K_{dc}	T_{1c}	T_{2c}	T_{3c}	T_{4c}	3.7
		134.1158	13.9487	12.3751	1.7451	1.5531	0.2802	0.5056	
	PID type PSS	K_{p1c}	K_{I1c}	K_{d1c}	T_{11c}	T_{21c}	T_{31c}	T_{41c}	
		111.8589	10.1969	48.8007	1.559	0.4859	0.1774	1.6069	
MFO	PID type SSSC	K_{pc}	K_{Ic}	K_{dc}	T_{1c}	T_{2c}	T_{3c}	T_{4c}	3.2
		469.7830	3.2563	18.4041	1.4773	1.6225	1.1597	1.7668	
	PID type PSS	K_{p1c}	K_{I1c}	K_{d1c}	T_{11c}	T_{21c}	T_{31c}	T_{41c}	
		0.9990	40.4269	2.4261	0.7406	1.8584	1.8608	1.8763	

5.4. Case-4: Fractional PID type SSSC and PSS controller

The nominal loading at ($P_e = 0.8, \delta_0 = 48.4^0$) line outage disturbance is at Bus-1. The proposed fractional PID type SSSC and PSS controllers have been implemented in this work to show their better quality over all the controllers. The transient analysis is done for the line outage disturbances of SMIB test system at nominal loading. The disturbance is created at 1 sec at one of the double circuit transmission line for 5 cycles and simulation results are studied from the Fig. 19-22 for speed deviation, tie line active power, terminal voltage and SSSC injected voltage, respectively. The settling time, overshoot and undershoot of the transient responses are improved effectively with this proposed controller as shown in Table 4. The time delay of 50 m sec is introduced between the FOPID type SSSC and PSS. Optimized with MFO algorithm, the proposed controller significantly improves the transient response as compared to DE optimized FOPID type SSSC and PSS controller and all other controllers.

Table 4 Case-4: DE and MFO tuned optimal parameter of FOPID type SSSC and PSS controller with nominal loading $(0.8 p.u, \delta_0 = 48.48^0)$, line outage

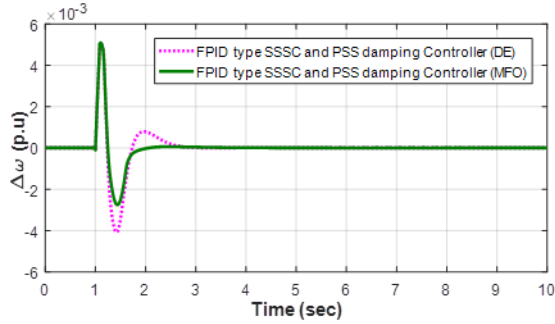| Optimisation	Controller	Controller Parameters									ITAE *10e-3
DE	FPID type SSSC	k_p 294.7739	k_I 54.5911	k_d 16.8004	T_1 0.5892	T_2 1.1404	T_3 1.6048	T_4 0.7965	λ 0.6887	μ 0.9087	3.4
	FPID type PSS	k_{p1} 57.7629	K_{I1} 11.4368	k_{d1} 31.4137	T_{11} 0.2451	T_{21} 1.3925	T_{31} 0.2039	T_{41} 0.9830	λ_1 0.4103	μ_1 0.9008	
MFO	FPID type SSSC	K_P 100.2096	K_I 37.6333	K_d 8.6803	T_1 1.8305	T_2 1.9974	T_3 1.5018	T_4 1.7566	λ 1.0185	μ 0.9987	2.9
	FPID type PSS	K_{P1} 161.2293	K_{I1} 94.0954	K_{d1} 27.9560	T_{11} 0.0920	T_{21} 0.0001	T_{31} 0.5633	T_{41} 1.4125	λ_1 1.1644	μ_1 1.1644	

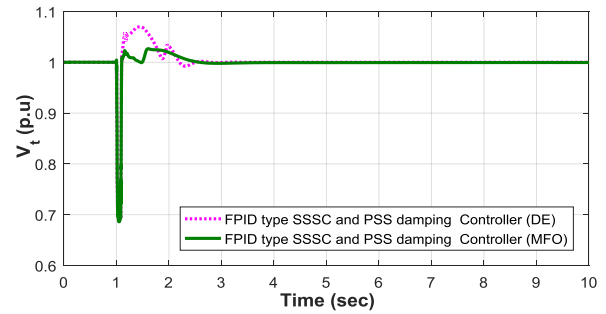
Fig. 19 Speed deviation

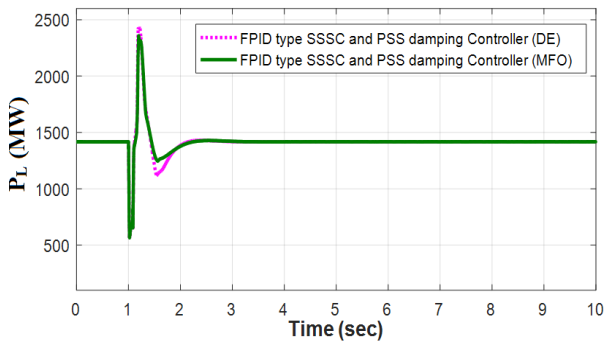Fig. 20 Terminal voltage

Fig. 21 Tie line active power
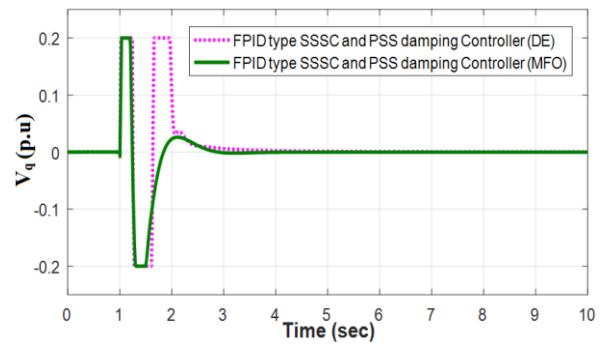

Fig. 22 SSSC-injected voltage controller

5.5 Case-5: Fractional PID type SSSC and PSS controller

The nominal loading at $(0.8 p.u, \delta_0 = 48.48^0)$ line outage disturbance is between Bus-2 and Bus-3. The MFO optimized speed responses of all the controllers are taken together in Fig. 23 and revealed that, the fractional PID with fractional number of integral gain and derivative gain effectively improves the dynamic responses as compared to rest of the controllers. The zoom portion of speed deviation shown in Fig. 24 clearly shows the speed response has no second overshoot, undershoot is less and it takes 2 sec to settle for damping out the complete oscillations.
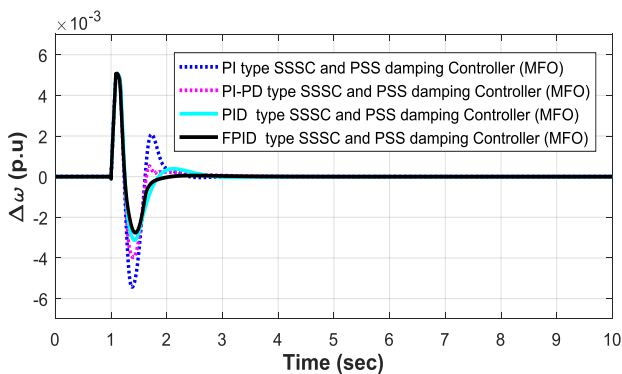

Fig. 23 Speed deviation for different controllers compared with proposed FOPID type SSSC and PSS controller
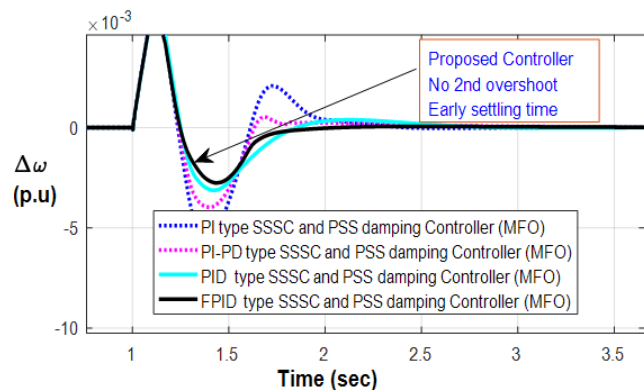

Fig. 24 Speed deviation in zoom version

5.6. Case-6: FOPID type SSSC and PSS controller nominal loading, permanent line tripping

Under severe disturbance condition, the proposed controller is verified at nominal loading. A three phase fault for 5 cycles is created at the mid-point of the overhead line of Bus-2 and Bus-3 and the fault is cleared by indefinite tripping of the faulted section. The responses of the system are shown in the Figs. 25-27. The speed deviation is shown in Fig. 25 in p.u, the rotor angle in deg in Fig. 26, and the healthy line power P_{L2} in MW in Fig. 27, respectively. The system responses are unstable without the controller and becomes stable by FOPID type SSSC type PSS damping controller. This controller brings the initial operating point of the speed deviation at 3 sec and the rotor angle in Fig. 26 is shifted to another operating point at $60°$ from its initial angle of $48.48°$ after 2.6 sec.
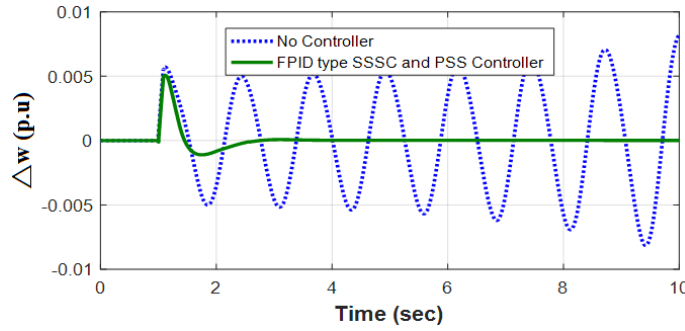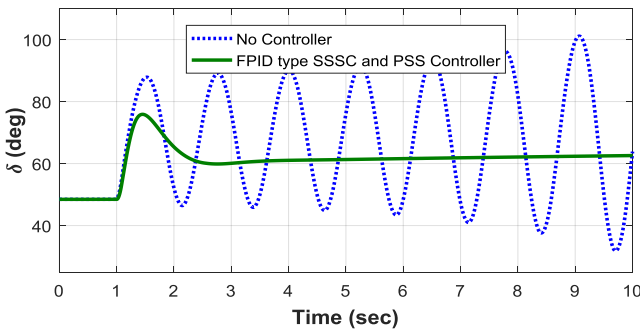

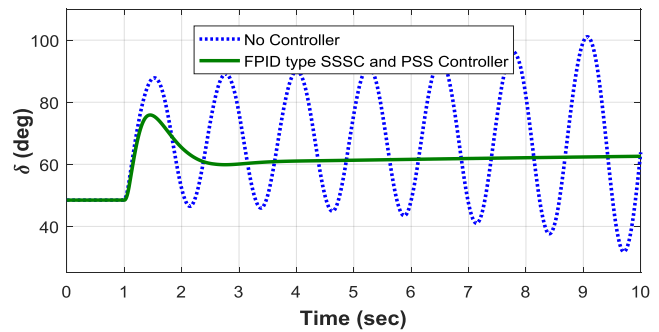Fig. 25 Speed deviation in p.u.

Fig. 26 Rotor angle in degree

Fig. 27 Power at healthy line

5.7. Case-7: FPID type SSSC and PSS controller

With light loading $(0.4 p.u, 22.85^0)$ and self-clearing, light load performances are also performed by changing the generator loading and the stability of the SMIB system is checked with the proposed FPID type SSSC and PSS damping controller. The responses are shown in the Fig. 28-30 with three phase fault for 5 cycles at middle of the double transmission line. The rotor angle in Fig. 29 *reduces* 22.85^0 (*without controller*) *to* 22.5^0 (*with controller*) and settling time is achieved at 3 sec. The effectiveness of this proposed controller is also verified in Figs. 28, 30 and 31 by showing the damping of the oscillations and reduced overshoot and undershoot after the first swing.
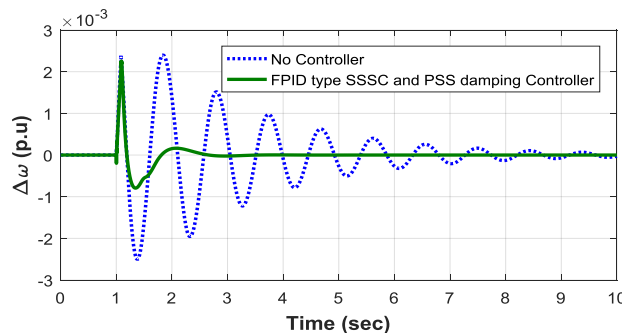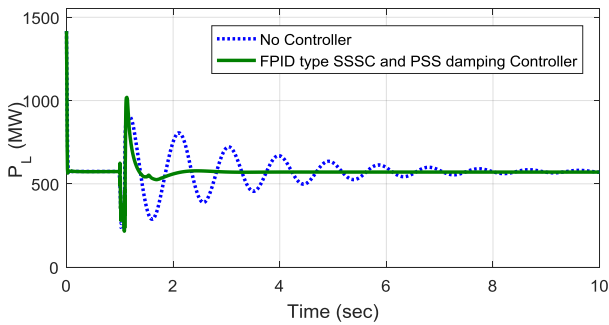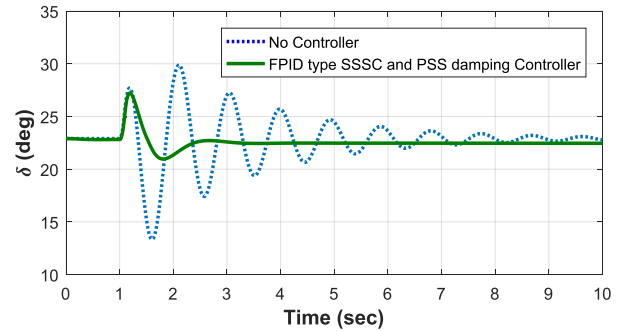

Fig. 28 Speed deviation

Fig. 29 Rotor angle

Fig. 30 Tie line Powerin MW

6. Conclusions

The main purpose here is to damp the power system oscillations and to enhance the system performance under disturbances. The coordinated PI, PI-PD, PID and FPID type SSSC and PSS damping controllers are designed and implemented in SMIB power system. The performance of Fractional PID type SSSC and PSS has been compared with other controllers by its ITAE based on speed deviation of the test system and found minimum ITAE as objective function. With optimizing the controller parameters by MFO, the robustness and effectiveness are verified under various contingencies. The system damping has also been compared by using proposed controller with DE, and has concluded that the MFO technique yields better ITAE value and better dynamic response. The simulation work has been done in MATLAB environment by running several times with adjusting controlling variables F= 0.5-0.8, CR= 0.5-0.8, strategy=1-3, iteration, populations and the range of other controller parameters within its limit in DE technique. Results obtained are good. However, in the proposed controller, 50 iterations, 10 population, F=0.8, CR=0.8, strategy=3 are considered and much better result are obtained. Similarly, 5 agents and 50 iterations are taken for MFO technique for still better results as compared to DE in this proposed test systems.

The results indicate the effectiveness of the proposed designs in providing good damping characteristics to power system oscillations. This also helps in enhancement of dynamic performance. This approach can be implemented with multi-machine grid connected power systems.

References

[1] S. Mirjalili, "Moth-flame optimization algorithm: A novel nature-inspired heuristic paradigm," Knowledge-Based System, vol. 89, pp. 228-249, November 2015.
[2] S. M. H. Hosseini, H. samadzadeh, J. Olamaei, and M. Farsadi, "SSR mitigation with SSSC thanks to fuzzy control," Turkish Journal of Electrical Engineering & Computer Sciences, vol. 21, pp. 2294-2306, January 2013.
[3] M. Klein, G. J. Rogers, and P. Kundur, "A fundamental study of inter-area oscillation in power systems," IEEE Press, August 1991, pp. 914-921.
[4] C. Liu, G. Cai, and D. Yang, "Design nonlinear robust damping controller for static synchronous series compensator based on objective holographic feedback-H," Journal of advances in Mechanical Engineering (Sage Journal), vol. 8, no. 6, pp. 1-11, June 2016.
[5] M. Bongiorno, J. Svensson, and L. Angquist, "On control of static synchronous series compensator for SSR mitigation," IEEE Transactions on Power Electronics, IEEE Press, June 2007, pp. 735-743.
[6] L. Bangjun and F. Shumin, "A brand new nonlinear robust control design of SSSC for transient stability and damping improvement of multi-machine power systems via pseudo-generalized Hamiltonian theory," Control Engineering Practice, vol. 29, pp. 147-157, August 2014.
[7] U. Q. Sun, Y. K. Sun, and X. X. Liu, "H2/HN cost-guaranteed control for the static synchronous compensator," IET Control Theory, vol. 69, pp. 641-646, 2009.

[8] M. S. Castro, H. M. Ayres, V. F. da Costa, and L. C. P. da Silva, "Impacts of the SSSC control modes on small-signal and transient stability of a power system," Electrical Power System Research, vol. 77, no. 1, pp. 1-9, January 2007.

[9] M. A. Abido, "Pole placement technique for PSS and TCSC based stabilizer design using simulated annealing," International Journal of Electrical Power Systems Research, vol. 22, no. 8, pp. 543-554, November 2000.

[10] M. E. About-Ela, A. A. Sallam, J. D. McCalley, and A. A. Fouad, "Damping controller design for power system oscillations using global signals," IEEE Transactions on Power Systems, IEEE Press, May 1996, pp. 767-773.

[11] M. A. Abido, "Optimal design of power system stabilizers using particle swarm optimization," IEEE Trans Energy Convers, IEEE Press, November 2002, pp. 406-413.

[12] Z. L. Gaing, "A particle swarm optimization approach for optimum design of PID controller in AVR system," IEEE Trans Energy Convers 19, IEEE Press, May 2004, pp. 384-391.

[13] S. Panda, "Robust coordinated design of multiple and multi-type damping controller using differential evolution algorithm," International Journal of Electrical Power & Energy Systems, vol. 33, no. 4, pp. 1018-1030, May 2011.

[14] H. E. Mostafa, M. A. El-Sharkawy, A. A. Emary, and K. Yassin, "Design and allocation of power system stabilizers using the particle swarm optimization technique for an interconnected power system," International Journal Electrical Power Energy Systems., vol. 34, no. 1, pp. 57-65, January 2012.

[15] T. T. Nguyen and R. Gianto, "Application of optimization method for control co-ordination of PSSs and facts devices to enhance small-disturbance stability," Proc. IEEE PES Transmission & Distribution Conf. May Dallas, IEEE Press, May 2006, pp. 21-24.

[16] Y. Li and K. H. Ang, "PID control system analysis and design," IEEE Control Systems. Magazines, IEEE Press, June 2005, pp. 559-576.

[17] C. H. Lee and F. K. Chang, "Fractional-order PID controller optimization via improved electromagnetism-like algorithm," Expert Systems With Application, vol. 37, no. 12, pp. 8871-8878, December 2010.

[18] F. Padula and A. Visioli, "Tuning rules for optimal PID and fractional-order PID controllers," Journal of Process Control, vol. 21, no. 1, pp. 69-81, January 2011.

[19] R. K. Khadanga and J. K. Satapathy, "Time delay approach for PSS and SSSC based coordinated controller design using hybrid PSO-GSA algorithm," International Journal of Electrical Power and Energy Systems, vol. 71, pp. 262-273, October 2015.

[20] S. S. Mohamed, A. E. Mansour, and M. A. Abdel Ghany, "Design of fractional order PID controller for SMIB power system with UPFC tuned by multi-objectives genetic algorithm," Proc. 16th Int. Conf. On Aerospace sciences & Aviation technology, pp. 26-28, May 2015.

[21] M. R. Faieghi and A. Nemati, "On fractional-order PID design, applications of MATLAB in science and engineering," Book Edited by Prof. Tadeusz Michalowski, pp. 237-292, September 2011.